# Water Splitting Mechanism on 2D Catalytic Materials

*DFT based Theoretical Investigations*

JOHN WÄRNÅ

Dissertation presented at Uppsala University to be publicly examined in Room Å80101, Ångströmlaboratoriet, Lägerhyddsvägen 2, Monday, 27 May 2019 at 13:15 for the degree of Doctor of Philosophy. The examination will be conducted in English. Faculty examiner: Naurang Saini (Sapienza University of Rome).

**Abstract**
Wärnå, J. 2019. Water Splitting Mechanism on 2D Catalytic Materials. DFT based Theoretical Investigations. *Digital Comprehensive Summaries of Uppsala Dissertations from the Faculty of Science and Technology* 1804. 57 pp. Uppsala: Acta Universitatis Upsaliensis. ISBN 978-91-513-0646-9.

In this thesis, we have envisaged systematic investigation to predict the water splitting mechanism on ultra-thin two-dimensional (2D) materials using cutting edge computation. Three different families of materials are considered as the case studies - i.$MX_2$ (where M= W and Pt) based transition metal dichalcogenides, ii. lightest 2D material as Boron monolayer and iii. $Mg_3N_2$ monolayer. The catalytic reaction mechanism of water dissociation consists of hydrogen evolution reaction (HER) and oxygen evolution reaction (OER), both of which are required to be investigated thoroughly in order to perceive the complete picture of water splitting. This is because of the fact that the fundamental understanding of how and why the improved solar hydrogenproduction properties could be developed for such 2D materials is also of great technological importance. We have performed rigorous electronic structure calculations based on density functional theory (DFT) to find the optimum catalytic activity of the considered monolayer nanostructures. Hydrogen and oxygen evolution reaction activity are determined from the surface-adsorbate interaction based on the adsorption energy of the major intermediates of HER and OER mechanism. Our DFT based investigations will be the intuitive way to theoretically rationalize HER and OER activity for a series of functionalized different two-dimensional systems and can guide the actual experiment in the laboratory with a preconceived framework.

*John Wärnå, Department of Physics and Astronomy, Materials Theory, Box 516, Uppsala University, SE-751 20 Uppsala, Sweden.*

*To my family and friends.*

# List of papers

This thesis is based on the following papers, which are referred to in the text by their Roman numerals.

I   **A comparative study of hydrogen evolution reaction on pseudo-monolayer WS2 and PtS2: insights based on the density functional theory**
S. Mir, S. Chakraborty, **John Wärnå**, S. Narayan, P. C. Jha, P. K. Jha, R. Ahuja
*Catalysis Science and Technology, 7, 687 (2017)*

II  **Two-dimensional boron: Lightest catalyst for hydrogen and oxygen evolution reaction**
S.Mir, S. Chakraborty, P. C. Jha, **John Wärnå**, H. Soni, P. K. Jha, R. Ahuja
*Applied Physics Letters, 109, 053903 (2016)*

III **Toward the Realization of 2D Borophene Based Gas Sensor**
V. Shukla, **John Wärnå**, N. K. Jena, A. Grigoriev, Rajeev Ahuja
*Journal of Physical Chemistry C, 121, 28169 (2017)*

IV  **Reaction Coordinate Mapping of Hydrogen Evolution Mechanism on $Mg_3N_2$ Monolayer**
**John Wärnå**, A. Banerjee, S. Chakraborty, R. Ahuja
*Manuscript Submitted*

Reprints were made with permission from the publishers.

The following papers are co-authored by me but not included in the thesis:

- **A computational study of potential molecular switches that exploit Baird's rule on excited-state aromaticity and antiaromaticity**
  H. Löfås, B. O. Jahn, **John Wärnå**, R. Emanuelsson, R. Ahuja, A. Grigoriev, H. Ottosson
  *Faraday Discuss., 174, 105-124 (2014)*

- **Sub 20 nm metal-conjugated molecule junctions acting as a nitrogen dioxide sensor**
  I. H. Wani, S. H. M. Jafri, **John Wärnå**, A. Hayat, H. Li, V. Shukla, A. Orthaber, A. Grigoriev, R. Ahuja, K. Leifer
  *Nanoscale 11, 6571 (2019)*

- **Mechanical properties of single-wall ZrO2 nanotubes: A finite element approach**
  X. Yang, H. Li, M. Hu, Z. Liu, **John Wärnå**, R. Ahuja, Yuying Cao and W.Luo
  *Physica E 98, 23 (2018)*

# Contents

# 1. Introduction

The monotonic growth of human population and the associated high living standards lead to the enormous energy demand. The increasing burning of fossil fuels to fulfill the energy demand causes pollution and the ever growing threat of the green house problem with temperature rice and melting polar ices are the inevitable consequences. There are alternatives like wind and water power, but they only stand for a small part of the energy production in the world. [1] Although there is nuclear power to resolve the energy demand, but the adverse effect of nuclear waste can not be ignored. The electrical energy storage needs to be maintained adequately with the demand constantly. One important solution is to use hydrogen as the energy carrier, which can be produced during the water splitting process. Hydrogen can easily be stored in metals [2, 3] and produced through photocatalytic water splitting under the visible light irradiation. [4]

An efficient water splitting process requires a highly catalytic material to expedite the process. The suitable photocatalyst for complete water splitting, that consists of hydrogen evolution reaction (HER) [5] and oxygen evolution reaction (OER) [6], requires an optimum band gap. [7] The two-dimensional (2D) nanostructured materials are good candidates for photocatalytic material with a good surface to volume ratio and also a tunable band gap. These 2D materials have become the promising candidates in recent years and are successfully synthesized, specially since the exfoliation of graphene (boron nitride, borophene, silicene etc.). [8–10] The advancement of computational material science together with the cutting edge experimental technique, it has become possible to modulate and predict new materials, with a range of vivid crystal structures and novel properties. The new materials can be functionalized with different doping elements to change the characteristics of properties like band gap, workfunctions, photoabsorption and also the associated adsorption energies of hydrogen and oxygen. A fundamental understanding of how and why improved catalytic properties can be developed for ultrathin pristine and functionalized 2D materials is of great technological importance from the perspective of efficient of hydrogen generation. This is the prime motivation behind this thesis, that has included the systematic investigation of nanostructured 2D materials for water splitting reaction mechanism. We have rigorously performed the electronic structure calculations based on Density functional theory (DFT) on intuitively chosen monolayers such as $PtS_2$, $WS_2$,

Boron and $Mg_3N_2$ sheet. The systematic electronic structure calculations have been used to determine the catalytic activity of the considered 2D materials based on adsorption free energies and the corresponding reaction coordinate. The catalytic activities associated with both HER and OER on such 2D materials have been envisaged along with the determination of functionaization effect on the respective systems. In this connection, we have constructed this thesis while distributing our findings in different chapters as described below.

Chapter 1 is the introduction and overview of photocatalytic water splitting [7] and how it relates to the energy production.

In Chapter 2, the theoretical background DFT framework has been explained. We start from the many-body theory and the Born-Oppenheimer approximation and Kohn-Sham ansatz [11], that are all finally leading to DFT formalism. The fundamental concepts behind the approximations like Exchange-correlation functional [12, 13], Projector Augmented Wave (PAW) method [14**?** ], Hybrid functionals [15–19], which are all extremely essential to perform electronic structure calculations with sufficient accuracy, are all explained.

In Chapter 3 the mechanism for Photocatalytic water splitting has been explained elaborately [4] The theory and principles of Hydrogen evolution reaction (HER) [5] and Oxygen evolution reaction (OER)[6] on 2D materials are described with a couple of case studies as $PtS_2$, $WS_2$ and Boron monolayers. At the end of the chapter, we provide the insight of photocatalytic water splitting together with the methodology based on DFT calculations [20–22] and finally we summarize the chapter.

Chapter 4 is dedicated to the obtained results of catalytic reaction mechanism of $PtS_2$, $WS_2$, Boron and $Mg_3N_2$ monolayer, with the associated discussion on workfunction, Density of states (DOS), absorption cross-section, adsorption energies and the reaction coordinate mapping. We have also highlighted the sensing application of Boron Monolayer from the perspective of electronic structure tuning, which interestingly following the similar motivation behind catalytic activity as well.

Chapter 5 will consist of Summary and Conclusion of the theoretical work on $PtS_2$, $WS_2$, Boron and $Mg_3N_2$ monolayer with a future outlook about the novel 2D energy materials worth to be investigated further.

A Swedish summary of the popular science regarding the importance of energy materials is depicted in Chapter 6.

In Chapter 7, I would like to acknowledge important people, who help me along the way.

# 2. Theoretical Foundation

## 2.1 The Many-Body problem

We are dealing with many atoms, while investigating electronic properties of materials in the form of bulk, surfaces, monolayers etc. Even the simplest system may contain substantial number of electrons as they consist of several number of atoms. In order to consider such a large number of electrons to determine the corresponding material's properties, we need to solve the associated many body problem, where we construct the Hamiltonian, $\hat{H}$, and subsequently solve the Schrödinger equation.

The Schrödinger equation can be expressed in the following form

$$\hat{H}\Psi = E\Psi \tag{2.1}$$

where the Hamiltonian is taken the following form:

$$\hat{H} = \hat{T}_e + \hat{T}_n + \hat{V}_{nn} + \hat{V}_{ee} + \hat{V}_{ne} \tag{2.2}$$

The first two terms of the Hamiltonian are the kinetic energy of the electrons and nucleus respectively. The next three terms are the Coulomb-like interactions between the nuclei, electrons and nucleus-electrons.

The Hamiltonian can also be expressed as the following:

$$\hat{H} = -\frac{\hbar^2}{2m_e}\sum_i^{N_e}\nabla^2 - \frac{\hbar^2}{2}\sum_k^{N_n}\frac{\nabla^2}{M_k}$$
$$+\frac{1}{2}\sum_{i\neq j}^{N_e}\frac{e^2}{|\mathbf{r}_i - \mathbf{r}_j|} + \frac{1}{2}\sum_{k\neq l}^{N_n}\frac{Z_k Z_l e^2}{|\mathbf{R}_k - \mathbf{R}_l|} - \sum_{i,k}^{N_e,N_n}\frac{Z_k e^2}{|\mathbf{r}_i - \mathbf{R}_k|} \tag{2.1}$$

where i, j indices are for the electrons and k, l are denoting different nucleus. $Z_k$ and $Z_l$ are the atomic number of the nucleus, $m_e$ and $M_k$ are the mass of the electron and the different nucleus.

## 2.2 Born-Oppenheimer approximation

The Schrödinger equation can only be solved exactly for the simplest and lightest element hydrogen (that consists of one proton and one electron). The

equation is getting complicated to be solved exactly for the second lightest element. To resolve this issue, Born-Oppenheimer approximation has been evolved, which says that the nucleus are much heavier than the electrons and therefore we can treat them as stationary with respect to the electrons. For this reason we can divide the equation in two parts one for the nucleus and one for the electrons. The effect of the nucleus can be added as an external potential $\hat{V}_{ext}$ when solving the electronic part of the equation.

$$\hat{H} = -\frac{\hbar^2}{2m_e}\sum_i^{N_e}\nabla^2 + \frac{1}{2}\sum_{i\neq j}^{N_e}\frac{e^2}{|\mathbf{r}_i - \mathbf{r}_j|} + \hat{V}_{ext}. \qquad (2.3)$$

## 2.3 Hohenberg-Kohn Theorems

In connection with the previously mentioned approximations, we need to determine the effect of all the electrons. Instead of calculating all the electrons interacting with each other, Hohenberg and Kohn proposed the concept of electron density $\rho_0(\mathbf{r})$ within the framework of density functional theory (DFT) [23]. Now we can calculate the external potential as follows from the theorems:

1. The ground-state electron density $\rho_0(\mathbf{r})$ determines the external potential $V_{ext}(\mathbf{r})$ for a system of interacting particles.
2. For any external potential, there exists a universal energy functional $F[n]$. The minimum value of the energy functional for a specific external potential $V_{ext}(\mathbf{r})$ is the ground state energy where the density that minimizes the functional is the ground state density $\rho_0(\mathbf{r})$.

The potential of the system only depends on the electron density and the ground state electron density is the minimum of the energy functional.

## 2.4 Kohn-Sham Ansatz

According to Kohn-Sham ansatz, the ground state energy of a system can be expressed as:

$$E_0[\rho(\mathbf{r})] = T[\rho(\mathbf{r})] + \int V_{ext}(\mathbf{r})\rho(\mathbf{r})d\mathbf{r} + \frac{1}{2}\iint \frac{\rho(\mathbf{r})\rho(\mathbf{r}')}{|\mathbf{r}-\mathbf{r}'|}d\mathbf{r}d\mathbf{r}' + E_{xc}[\rho(\mathbf{r})] + E_{II},$$
(2.4)

Since all the electrons are affected by the charge density instead of interacting with the other electrons, we can let every electron have its own eigenfunction, the Kohn-Sham eigenfunction $\psi_i$. Subsequently, we determine an effective potential, $V_{eff}$ and the eigenfunctions $\psi_i$.

$$\left\{ -\frac{1}{2}\nabla^2 + V_{eff}(\mathbf{r}) \right\} \psi_i(\mathbf{r}) = \varepsilon_i \psi_i(\mathbf{r}),$$
(2.5)

$$\rho(\mathbf{r}) = \sum_{i=1}^{N} |\psi_i(\mathbf{r})|^2$$
(2.6)

From the above, we can determine the corresponding electron density and the effective potential. Equation 2.5 and 2.6 are solved self-consistently until we eventually find the ground state energy of the system. [11]

## 2.5 Exchange-Correlation Functional

The effective potential of Equation 2.5 can be divided into three parts as $V_{eff} = V_{Hartree} + V_{ext} + V_{xc}$, where $V_{Hartree}$ and $V_{ext}$ can be calculated exactly. The $V_{xc}$ term is still unknown, therefore we need some approximations to use Equation 2.5 properly. The two most widely used exchange-correlation functionals are Local Density Approximation (LDA) and Generalized Gradient Approximation (GGA). The LDA functional uses the electron gas of interacting particles as an approximation for the exchange and correlation functional according to Equation. 2.7. It might still work fine for different systems, however it tends to underestimate the lattice parameters and band gap and overestimate binding energies. In systems, where LDA does not work reasonably good, GGA has been proposed as an alternative for exchange and correlation functional. The GGA functional employs not only the electron density in every point but also the rate in which the density varies (the gradient) according

to Equation. 2.8. The GGA functional improves the accuracy for different physical properties, as energies and lattice parameters. The GGA functional itself can be describes in different ways according to Becke, Perdew, Wang or Ernzerhof for example. [12] [13]

$$E_{xc}^{LDA}[\rho(\mathbf{r})] = \int_{\mathbf{r}} \varepsilon_{xc}(\rho)\rho(\mathbf{r})d\mathbf{r} \tag{2.7}$$

$$E_{xc}^{GGA}[\rho(\mathbf{r})] = \int_{\mathbf{r}} \varepsilon_{xc}(\rho, \nabla\rho)\rho(\mathbf{r})d\mathbf{r} \tag{2.8}$$

## 2.6 Projector Augmented Wave (PAW) formalism

Considering all the aforementioned approximations and correlations, the electronic structure calculations are still computationally expensive. One way to decrease the computing time is to use the projected augmented wave (PAW) formalism. This method uses a smooth wave function describing the electrons near the nucleus; the core region (C). This can be done in a good agreement with theory because it is only the valence electrons overlapping to neighbouring atoms. A real description of the core electrons is a fast oscillating wave function, which would require many wave functions to make up for the total Fourier transformation. Instead, the PAW method uses pseudo wave functions, which are transformed by an operator $\hat{T}$ into the real Kohn-Sham single particle wave functions. [24] [14]

$$|\psi\rangle = \hat{T}|\psi'\rangle \tag{2.9}$$

where $|\psi\rangle$ is the real single particle wave function and $|\psi'\rangle$ is transformed the pseudo wave function. We can construct the operator $\hat{T}$ by considering that the wave functions have to be the same outside the core region. Inside the core region, it is possible to construct this region with smoother partial waves.

$$|\Psi'\rangle = \sum_i |\phi_i'\rangle c_i \tag{2.10}$$

17

We can write the total single particle wave function inside and outside the core region as Equation. 2.11 where $T_C$ only acts inside C.

$$|\Psi\rangle = \sum_i |\phi_i\rangle c_i = \hat{T} |\Psi'\rangle \tag{2.11}$$

$$\hat{T} = 1 + \sum_C T_c \tag{2.12}$$

$$c_i = \langle \hat{p}_i | \Psi' \rangle \tag{2.13}$$

$$\langle \hat{p}_i | \phi_j' \rangle = \delta_{ij} \tag{2.14}$$

$$\sum_i |\phi_i'\rangle \langle \hat{p}_i| = 1 \tag{2.15}$$

$$T_C |\Psi'\rangle = \sum_i T_C |\phi_i'\rangle c_i = \sum_i (|\phi_i\rangle - |\phi_i'\rangle) \langle \hat{p}_i | \Psi' \rangle \tag{2.16}$$

$$\hat{T} = 1 + \sum_i (|\phi_i\rangle - |\phi_i'\rangle) \langle \hat{p}_i| \tag{2.17}$$

The transformation of the pseudo wave functions into real functions has to be linear. This means that it is possible to project the coefficients from the operators $\hat{p}_i$ according to Equation. 2.13, if we consider that Equation. 2.14 and 2.15 define the operators $\hat{p}_i$, while using Equation. 2.10 and 2.13, we finally end up with Equation. 2.16 within the core region with Equation. 2.17 originates from Equation. 2.9.

We have used Vienna Ab-initio Simulation Package (VASP) for performing the rigorous electronic structure calculations in this thesis-work, which is based on the formalism of PAW method together with pseudo-potentials for each element in the structure. In the pseudo-potentials, the nuclear charge is screened by the core electrons, which is a good approximation since only the valance electrons are responsible for the interatomic interactions.

## 2.7 Hybrid Exchange Correlation Functional

In case of band gap determination of bulk or surface systems, the accuracy provided by the exchange correlation approximation such as LDA and GGA are not sufficient. To resolve this issue, different approaches have been taken into consideration, with different mixing of non local Hartree-Fock exchange and local exchange correlation, while mixing of exact and approximated functional. Few of such useful functionals are PBE0 (2.18) and Heyd-Scuseria-Ernzerhof (HSE 06) (2.19), where they both have different exchange and correlation terms.

$$E_{xc}^{PBEO} = \alpha E_x^{HF} + (1-\alpha)E_{xc}^{PBE} \tag{2.18}$$

$$E_{xc}^{HSE} = \alpha E_x^{HF,SR} + (1-\alpha)E_x^{PBE,SR} + E^{PBE,LR} + E_c^{PBE} \tag{2.19}$$

where $\alpha$ is the mixing parameter and SR and LR stand for short ranged and long ranged respectively [15] [16] [17] [18] [19].

## 2.8 Molecular Dynamics Simulation

We can determine atomic movement due to thermal energy in Molecular Dynamics (MD) simulation. The atomic displacement is because of the forces acting upon them,

$$F_i = M_i a_i \tag{2.20}$$

where $F_i$ and $a_i$ are the force and acceleration of the individual atom with mass $M_i$. In our works, we have used Born-Oppenheimer Molecular Dynamics [25], which allows us to determine the positions of the electrons and the nuclei separately. The self-consistent Kohn-Sham equations are solved for the electrons with the atoms at initial positions, and subsequently the forces acting on the nuclei are determined using Verlet algorithm [26]. This continues for a certain amount of time until the nuclei find the local minimum. The first step is to calibrate the system into thermal equilibrium and subsequently the simulation is performed to manifest the information for determining the material's properties. In this thesis, MD simulation has been used to determine the positions of the hydrogen atoms on the 2D material's surface. We also investigate the stability of the surface for the 2D material, while the atomic bindings within

the layer stay more or less constant, whereas the layer-hydrogen bindings are changing. We can relax the final structure to get the binding energy for HER once the system is in equilibrium with hydrogen adsorbate.

# 3. Photocatalytic Water Splitting Mechanism

## 3.1 Introduction

Nowadays, the biggest challenge for scientific community is to search for a sustainable solution to the growing energy demand and at the same time reduce the use of carbon based fuels. The idea of producing electricity using renewable energy sources like wind depends on the weather, as it will be high when the wind is blowing and low in the less presence of wind. Therefore, in order to exploit the full advantage of the energy produced, we will need clean, efficient, abundant, cheap and better ways to store such energy. The most promising solution to the problem is hydrogen production and the economical way to produce hydrogen is to split the water into oxygen and hydrogen (water splitting $H_2O \Rightarrow H_2 + O_2$). This process is an endothermic reaction, which requires an external source of energy. The easiest way would be electrochemical process, which was induced in 1972 by Fujishima and Honda while splitting the water into $H_2$ and $O_2$ based on a photoelectrochemical method. This method required a bias voltage to the electrodes, however it was shown in 1979 that while using a powder of $TiO_2$ with the sun as an energy source, it was possible to split the water without adding the bias. Since then, scientists have been trying to find better materials for this type of applications.

The hydrogen based energy is easily accessible (hydrogen can be part of many different reaction), it is produced by water, which is an abundant substance, has a great storage possibility in gas or liquid form or absorbed in metal hydrides. If done efficiently hydrogen will have an environmental, economical and social impact on the world. However, to be fully able to substitute the energy from carbon based fuels we have to make the production cheaper and more efficient, while thinking about the social implication and use catalyst material that will not harm us or future generations. To date the most efficient catalyst are noble metals, which of course are not abundant and expensive. With this in mind scientist still have some issues to resolve. The main process in the water splitting material is to create electron-hole pairs. This means that the material in question has to have a good electron gathering possibility. To be able to create electron-hole pairs we have to excite electrons from the valance band to the connection band, which creates electrons in the conduction band and holes in the valance band. If this is to be done by absorbing visible solar light, the band gap of the material needs to be optimum in order to absorb solar radiation frequency to excite the electrons. The

idea is to let electron-hole pairs react with the adsorbed water molecules on the surface, where they can start the Hydrogen Evolution Reaction or HER ($4H_2O + 4e^- \Rightarrow 4OH^- + 2H_2$), and the Oxygen Evolution Reaction or OER ($4OH^- + 4h^+ \Rightarrow O_2 + 2H_2O \Rightarrow 4H^+ + 4e^- + O_2$). This is possible if the electron-hole pairs can migrate to the surface of the material before they recombine. [4]

## 3.2 Hydrogen Evolution Reaction (HER)

To have a material "better" for HER, there are a few important aspects to look for in the search for a optimal catalyst. They are efficiency, durability and cost-effectiveness. First of all, we need to know the exchange current density, $i_0$, which is basically the rate in which $H_2$ forms from $H^+$ at equilibrium. Another important criteria is the Tafel slope, which is a measurement over the potential needed to increase the the current by one magnitude at the time of starting the reaction with the "onset potential" applied. An ideal HER catalyst should have high exchange current density and a low Tafel slope. Even if the material is optimal for HER with a substantial efficiency, but can not stand against the tide of time (if material is corroding or in another way contaminated) then the material still would not be a good choice for a HER catalyst. The total cost of a HER catalyst can be divided into two parts called "hard costs" and "soft costs". The first term is related to the price of the element and chemicals used in the process of making the material and the second is related to the synthetic manufacturing of the photo-catalyst. To have less expensive catalytic material, one can choose more abundant elements, elements with a low market price. The overall HER reaction, which is taking place at an electrode in contact with an electrolyte is consisting of three elementary reactions. The first step is mainly regarding the dissociation of $H_2$ and adsorbed hydrogen atom. It can be undergone in two ways, which are called Tafel route and Heyrovsky route. In Tafel route ($H_2 \rightarrow 2H^*$), $H^*$ denotes hydrogen adsorbed on the surface hydrogen adsorbed on the surface and in Heyrovsky way it is like $H_2 \rightarrow H^* + H^* + e^-$. This adsorbed hydrogen is discharged afterward which follows Volmer route $H^* \rightarrow H^+ + e^-$. Even on the most studied electrode material like Platinum, it is still not completely agreed, which of the two pathways, Tafel-Volmer or Heyrovsky-Volmer is favorable. Seeing these facts,
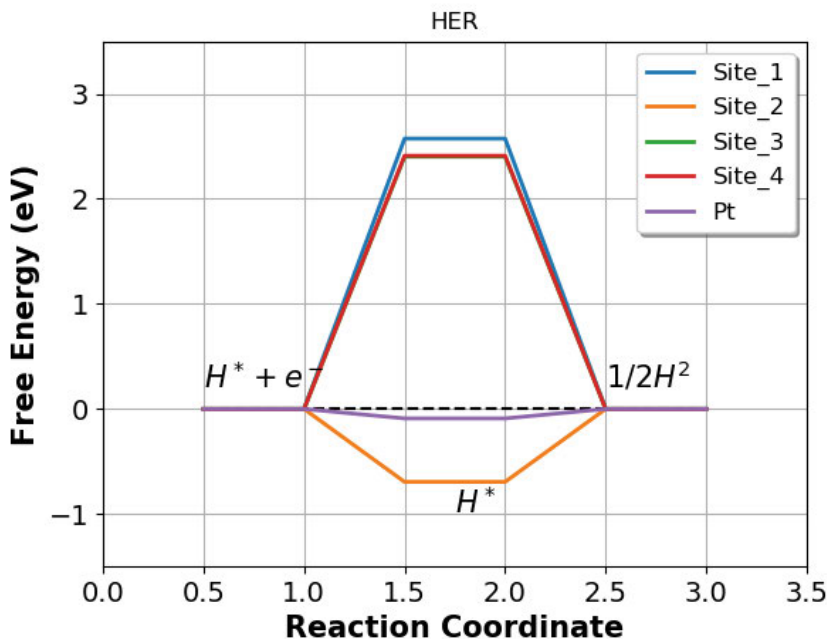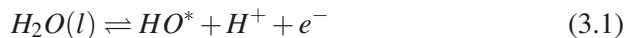
*Figure 3.1.* The figure shows the reaction coordinate for HER ( paper IV). $Site_1$, $Site_2$, $Site_3$ and $Site_4$ refer to hydrogen adsorption sites on a particular material.

the research interest is mainly revolving around modeling of electrochemical double layer at an electrode, which has to be done with more precision based on DFT simulations. Changing the number of protons/electrons in the double layer can be an intuitive investigation of the system as a function of electrode potential.

## 3.3 Oxygen Evolution Reaction (OER)

The oxygen evolution reaction (OER) in the counter-electrode, can be composed of four reaction steps, whereas at each step, there $H^+$ and $e^-$ pair are forming, and this is why this mechanism is called four electron pathway as follows (equations 3.1-3.4):

$$H_2O(l) \rightleftharpoons HO^* + H^+ + e^- \tag{3.1}$$

$$HO^* \rightleftharpoons O^* + H^+ + e^- \tag{3.2}$$

$$O^* + H_2O(l) \rightleftharpoons HOO^* + H^+ + e^- \tag{3.3}$$

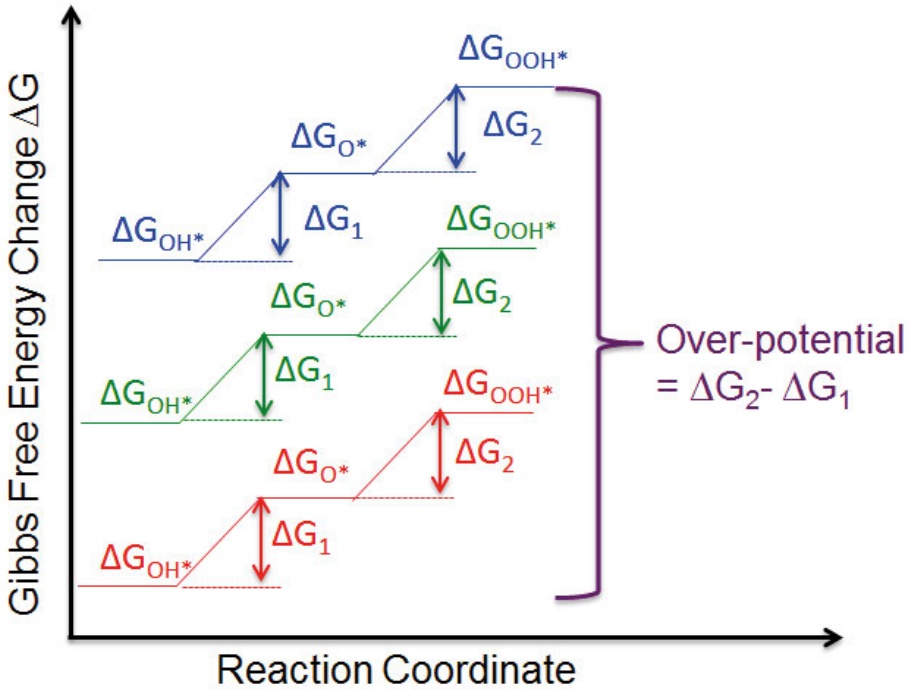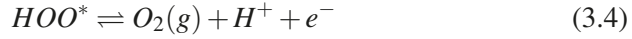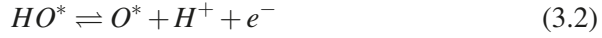$$HOO^* \rightleftharpoons O_2(g) + H^+ + e^- \tag{3.4}$$



*Figure 3.2.* The figure shows the reaction coordinate for Oxygen Evolution Reaction

The thermochemistry of these reactions can be explained by a previously developed model based on density functional calculation. These reaction steps are mainly followed in acidic medium. In presence of alkaline medium, the thermodynamic analysis and the intermediate products remain the same. However, in our calculations, we have considered the systems to be at pH=0. The potential required to remove proton and electron is determined by the change in adsorption free energy of the reaction intermediates. Thus minimization of the overpotential requires binding of the reaction intermediates to the catalyst surface with right strength. The total free energy for oxygen evolution is usu-

ally determined by the second step as it is the step with largest free energy change. Now If we know the overpotential for each step, then the free energy diagram or the reaction coordinate can easily be deduced.

## 3.4 Two-dimensional (2D) Catalytic Materials

The promising candidates for water splitting processes are semiconductors, they have the required band gap and 2D materials have large surface to volume ratio. Since the discovery of graphene, the 2D materials have been an attractive subject area for both theoreticians and experimentalists. In theory, one can determine new combinations of different species of atoms to build several types of 2D materials based on the DFT formalism, while the experimentalists can synthesize more and more of these kind of 2D materials. With the tools available in the DFT code we can now tailor several properties of materials and can see whether the material in question would be a good candidate for this application or not. DFT uses the electron density to calculate the most stable configuration of the system by comparing the total energy, the lower the energy the more stable the system is. If we compare different adsorbate on the pristine and functionalized 2D sheet (like $H_2O$ and the corresponding intermediates of HER and OER process), we can actually determine the adsorption free energy of $H^*$ in case of HER and $O^*$, $OH^*$, $OOH^*$ in case of OER and compared the values between pristine and functionalized monolayer to see the effect of substitutional and functionalization on the respective catalytic activity. The band gap can be obtained by evaluating the density of states (DOS). [7]

One of the recent advancements in exfoliation techniques is the synthesis of 2D transition metal dichalcogenides (TMDCs), having the structural formula $MX_2$ (where M is a transition metal and X = S, Se, and Te), which have been attracted significant attention because of their distinctive crystal structures and rich chemical diversity. For instance, several semiconducting TMDCs, such as $MoS_2$, $MoSe_2$, $WS_2$, and $WSe_2$, undergo an indirect to direct bandgap transition while going from bulk to monolayer. The relatively high mobility of charge carriers in TMDCs has opened up new avenues for employing these materials in a variety of applications

## 3.5 Role of DFT for Prediction of HER and OER Activities

The ability of a given surface to be a good HER catalyst is given by exchange current density, which can be related to the free energy of adsorbed hydrogen ($H_2$) when the reaction is at equilibrium. The free energy of hydrogen in the adsorbed state is defined as $\Delta G = E_{ads} + \Delta E_{ZPE} - T\Delta S$, where $E_{ads}$ is the adsorption energy of hydrogen, $\Delta E_{ZPE}$ represents the zero point energy (ZPE) difference of $H_2$ in the adsorbed state and the gas phase and $T\Delta S$ is the entropy of $H_2$. A good catalyst has $\Delta G$ is close to zero. To predict a good OER catalyst, it is important to have a low overpotential, which can be calculated as the difference between the adsorption energies of $HOO^*$ and $HO^*$ respectively, where * denotes that O is binding to the surface. These adsorption energies and consequently the adsorption free energies are calculated using Vienna Ab-initio Simulation Package (VASP) within the framework of DFT formalism. [20–22]

We have extensively used DFT to investigate the catalytic activity for the 2D materials in the thesis-work, which are revolving around (i) platinum disulphide (PtS$_2$) and tungsten disulphide (WS$_2$), functionalized with different dopants, (ii) boron monolayer, and (iii) $Mg_3N_2$ monolayer. We have changed the structural and electronic properties of the boron sheet by doping it with carbon, nitrogen, phosphorous, sulphur and lithium and PtS$_2$ and WS$_2$ with different transition metals like Ru, Rh, Pd, Aq, Ir, Au and Hg. We have determined the corresponding adsorption energies of hydrogen and oxygen to predict the activity of HER and OER, in addition to the determination of the density of states and optical absorption cross section. We have also envisaged $Mg_3N_2$ monolayer for HER activity while changing the concentration of hydrogen adsorption. After obtaining the adsorption energies, we construct the reaction coordinate for HER on the specific 2D systems, which eventually will measure the ability of the material as an efficient catalyst for hydrogen generation.

4. Efficient 2D Materials: $PtS_2$, $WS_2$, Boron and $Mg_3N_2$ monolayer

## 4.1 Two-dimensional PtS$_2$ and WS$_2$ Monolayers for HER and OER Mechanism

In this study, we have investigated the catalytic activity of ultrathin PtS$_2$ and WS$_2$ nanostructures for the hydrogen evolution reaction by electronic structure calculations based on the spin-polarized DFT. We have also explored the effect of van der Waals interactions on the surface adsorbate interactions. Using the adsorption free energy of hydrogen as an activity descriptor, we have tuned the photocatalytic water splitting activity of PtS$_2$ and WS$_2$ by functionalizing the individual systems with different transition metals such as Ru, Rh, Pd, Ag, Ir, Au, and Hg. The density of states has been calculated along with the band structure to find the effect of different dopants on the fundamental band gap, which is one of the primary parameters in the photocatalytic water splitting.

All the calculations of platinum disulphide (PtS$_2$) and tungsten disulphide (WS$_2$) were made with DFT in the VASP code. To describe the ion-electron interaction we used the PAW method and for the exchange-correlation terms we used the GGA functional based on the PBE form. To better describe the dispersive forces and correctly describe the adsorption energy we used (D3) of Grimme. The plane wave basis set had a energy cut-off at 500 eV. For the structural convergence criterion we used less than 0.02 eV/Å for the forces on the atoms and $1.0 \times 10^{-5}$ eV for the change in energy. All the adsorption energy calculations used $3 \times 3 \times 1$ supercell with an extra 22Å vacuum in the z-direction (including 27 atoms, 9 metal atoms and 18 S atoms). The optimization of the gas ($H_2$) adsorption were calculated using spin polarization. As a starting guess for bond distances the $H_2$ molecules were placed at distances 3-4.2Å from the metal layer. The Brillouin zone sampling used k-points in a $4 \times 4 \times 1$ k-mesh from the Monkhorst-Pack scheme. Band gap calculations were made using the hybrid HSE06 functional and the DOS was calculated with the GGA functional by a $8 \times 8 \times 1$ k-mesh. The crucial part of the HER activity calculation is $H_2$ adsorption energy on the catalyst surface. The $H_2$ adsorption energy or the adsorption free energy of $H_2$ ($\Delta G_H$) on the electrode is how the catalytic activity for the HER is described. The expression for the adsorption free energy is $\Delta G_H = E_{ads} + \Delta E_{ZPE} - T\Delta S_H$, where $E_{ads}$ is the adsorption energy for the $H_2$ molecule, $E_{ZPE}$ is the zero point energy difference of $H_2$ in the adsorbed and gas state and $T\Delta S_H$ is the entropy of the $H_2$ molecule in the

adsorbed and gas state. $\Delta E_{ZPE}$ for $H_2$ varies from 0.01-0.04 eV and $T\Delta S_H$ has an approximate value of 0.4 eV. The vibrational entropy is small for $H_2$ in the adsorbed state, so the adsorption entropy is 1/2 of $H_2$, $\Delta S_H \approx -1/2\Delta S_{H_2}$, where $\Delta S_{H_2}$ is the entropy of $H_2$ in the gas phase. An optimal HER catalyst has $\Delta G_H = 0$. If $\Delta G_H = E_{ads} + 0.24 = 0$, then $E_{ads}$ should be in the region of -0.24 eV. We used the formula $E_{ads} = E_{x+H_2} - E_x - E_{H_2}$ to evaluate the adsorption energy, where x represent the different pristine and functionalized catalyst materials versions of Pt$S_2$ and W$S_2$. We tried different sites for the $H_2$ adsorption to find the most probable adsorption.

The relaxed crystal structures of PtS$_2$ and WS$_2$ pseudo-monolayers are shown in Fig. 4.1. Pt and W are sandwiched between two layers of sulphur, where Pt- and W atoms have octahedral- and trigonal coordination symmetries. The sulphur atoms have hexagonal or rhombohedral symmetries respectively. The lattice constant for PtS$_2$ is 3.538 Å with a Pt-S bond length of 2.389 Å and the W-S bond length is 2.407 Å and WS$_2$ has a lattice constant of 3.146 Å. One of the most important descriptors for catalytic activity is the band gap of the material. In Fig. 4.1 (C) and (f) the band structure for PtS$_2$ and WS$_2$ is shown. PtS$_2$ is a semiconductor with an indirect band gap of 2.60 eV, where the valance band maximum (VBM) is situated at $\Gamma - K$ and the corresponding conduction band minimum (CBM) at $\Gamma - M$. WS$_2$ has a direct band gap of 2.14 eV. To tune the efficiency of photocatalytic activity, both systems were functionalized with 4d (Ru, Rh, Pd and Ag) and 5d (Ir, Au and Hg) transition metals. In Table 4.1 the calculated bond length of the dopants to the nearest neighbour sulphur atoms are shown. The largest deviation compared with the pristine PtS$_2$ and WS$_2$ was found for the Ag-, Au- and Hg-doped Pt$S_2$ systems, where the bond length increased with 0.21 Å and in the Pd-, Ag-, Au- and HG-doped WS$_2$ systems the increase was 0.22 Å. In all the other doped PtS$_2$ and WS$_2$ systems not much deviation was found. The workfunctions ($\Phi$) are displayed in Table 4.1.

In Fig. 4.2 the DOS for the pristine and doped system are plotted to see the effect on the band gap with respect to the functionalization. In the case of doped PtS$_2$ systems the dopants Au, Ag and Hg induce states inside the band gap near the Fermi level. It has been shown that the gap was shifted toward lower energy in comparison to pristine PtS$_2$. For the other systems neither ef-
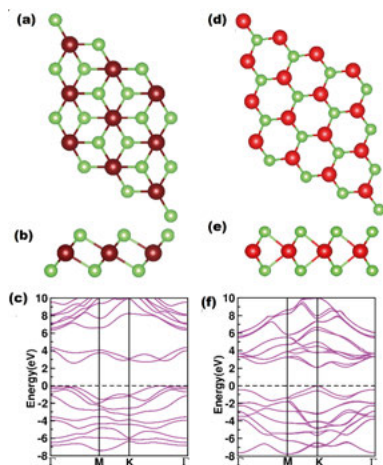
*Figure 4.1.* (a) and (b) show the crystal structure of $PtS_2$ in 1T phase, top- and side view respectively. (d) and (e) show the crystal structure of $WS_2$ in 2H phase, top- and side view respectively. (c) and (f) show the band structure of $PtS_2$ and $WS_2$. The colours of the element are green=S, brown=Pt and red=W.

fects were found. All the dopants shift the VBM toward more negative energy levels compared to the pristine $WS_2$ monolayer. The catalytic activity for the HER can be enhanced for $PtS_2$ and $WS_2$ monolayers do to the strong effect on the band gaps of $PtS_2$ and $WS_2$ from the dope atoms. Another important indicator to predict catalytic activity for the HER is hydrogen adsorption energy, which is calculated using the equation $E_{ads} = E_{system+H_2} - E_{system} - E_{H_2}$. $E_{ads}$ is the adsorption energy of the hydrogen gas, $E_{system+H_2}$ is the energy of the nanosheet with the adsorbed gas, $E_{system}$ is the energy of the nanosheet without the adsorbed gas and $E_{H_2}$ is the energy of the gas molecule. The adsorption energy was calculated for top and hollow sites of pristine and the functionalized pseudo-monolayers. Two configurations were considered, one with the where the bond axis of the hydrogen gas molecule was perpendicular to the surface of the material and one where the bond axis was parallel to the surface. The adsorption energies for the doped and pristine $PtS_2$ and $WS_2$ are presented in Table 4.2, where all the energies are calculated with and without van der Waals interaction included. In conclusion, when $WS_2$ was doped with Pd, the strength of the binding energy increased by an order of magnitude and made the hydrogen adsorption energy for this system optimal for the HER. [27–32]

| | PtS$_2$ | PtS$_2$ | WS$_2$ | WS$_2$ |
|---|---|---|---|---|
| **Impurity** | S-X(Å) | $\Phi(eV)$ | S-X(Å) | $\Phi(eV)$ |
| Pristine | 2.389 | 6.280 | 2.407 | 5.632 |
| Ru | 2.384 | 5.880 | 2.380 | 4.234 |
| Rh | 2.370 | 6.222 | 2.413 | 4.507 |
| Pd | 2.390 | 6.276 | 2.484 | 4.836 |
| Ag | 2.494 | 5.624 | 2.562 | 5.047 |
| Ir | 2.374 | 6.062 | 2.390 | 4.304 |
| Au | 2.483 | 5.200 | 2.572 | 4.894 |
| Hg | 2.601 | 5.482 | 2.626 | 5.198 |

**Table 4.1.** *Optimized bond lengths S-X (X is Pt, W from the pristine case and the dope atoms) and the workfunctions of the pristine and doped PtS$_2$ and WS$_2$.*

| | PtS$_2$ | PtS$_2$ | WS$_2$ | WS$_2$ |
|---|---|---|---|---|
| **Impurity** | Non-VDW | VDW | Non-VDW | VDW |
| Pristine | -0.0117$\perp$ | -0.0407$\parallel$ | -0.0109$\perp$ | -0.0654$\perp$ |
| Ru | -0.0118$\parallel$ | -0.0533$\parallel$ | -0.0079$\perp$ | -0.0647$\perp$ |
| Rh | -0.0153$\parallel$ | -0.0509$\perp$ | -0.008$\perp$ | -0.0736$\perp$ |
| Pd | -0.0100$\parallel$ | -0.0502$\perp$ | -0.0103$\perp$ | -0.232$\perp$ |
| Ag | -0.0689$\perp$ | -0.0543$\parallel$ | -0.0299$\parallel$ | -0.0664$\perp$ |
| Ir | -0.0119$\perp$ | -0.0533$\parallel$ | -0.0114$\perp$ | -0.0647$\perp$ |
| Au | -0.0143$\parallel$ | -0.0520$\perp$ | -0.0446$\parallel$ | -0.0666$\perp$ |
| Hg | -0.0181$\perp$ | -0.0556$\perp$ | -0.0114$\perp$ | -0.0668$\perp$ |

**Table 4.2.** *Adsorption energies (in eV) of H$_2$ on pristine and doped PtS$_2$ and WS$_2$. The symbols $\parallel$ or $\perp$ represent if the adsorption of H$_2$ is parallel or perpendicular*

## 4.2 Two-dimensional Boron Monolayer for HER and OER Mechanism

The hydrogen evolution reaction (HER) and oxygen evolution reaction (OER) have been envisaged on a two-dimensional (2D) boron sheet through electronic structure calculations based on DFT framework. To date, boron sheets are the lightest 2D material and, therefore, exploring the HER and OER activity of such a monolayer system would be quite intuitive both from fundamental and application perspectives. We have functionalized the boron sheet (BS) with different elemental dopants like carbon, nitrogen, phosphorous, sulphur, and lithium and determined the adsorption energy for each case. The free energy calculated from the individual adsorption energy for each functionalized
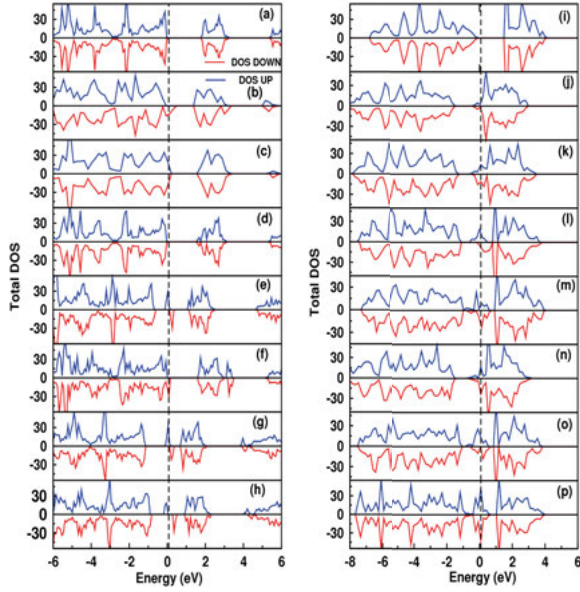
*Figure 4.2.* The left hand column shows the total DOS of pristine (a) and functional-ized $PtS_2$ (b)-(h). The right column shows the total DOS of pristine (i) and function-alized $WS_2$ (j)-(p). Both $PtS_2$ and $WS_2$ are functionalized with Ru, Rh, Pd, Ag, Ir, Au and H. Zero energy represents the Fermi level.

BS subsequently guides us to predict which case of functionalization serves better for the HER or the OER.

To calculate the structural optimizations, electronic and optical properties we employed DFT as implemented in VASP. The description of the core elec-trons and the ion-electron interaction were made using the PAW method. For the optimizations of the boron sheets (both pristine and functionalized) we used the PBE functional and the exchange and correlation contribution was described with GGA. A $25 \times 25 \times 1$ k-mesh integration within the Brillouin zone was used for the description in the Monkhorst-Pack scheme. Plane wave basis set with an energy cut-off of 500 eV were used for the valence electrons. The optimization ran until the Hellman-Feynman forces on the atoms were less than 0.02 eV/Å and the change in energy was less than $1.0 \times 10^{-5}$ eV. A larger k-mesh of $41 \times 41 \times 1$ k-points was used to calculate DOS and optical spectra. To avoid interaction with neighbouring images 30Å vacuum is added to the cell in the z-direction. To see the optical response i.e the adsorption spectra we used the following formula for the real and imaginary part of the

frequency-dependent dielectric function $\varepsilon(\omega) = \varepsilon_1(\omega) + i\varepsilon_2(\omega)$. The ability of a HER catalyst is measured by exchange current density, which can be related to $\Delta G_H$. The same formula can be used when you want to measure the ability of the material for OER. For $O_2$ the entropy difference is 0.63 eV, this leads to using the same reasoning that $\Delta G_O = E_{ads} + 0.33 = 0$. For the optimal OER catalyst $E_{ads}$ should be in the order of -0.33 eV. We calculated the adsorption energies for $H_2$ and $O_2$ on different sites for pristine and functionalized boron sheets. The adsorption energy, $E_{ads} = E_{system+gas} - E_{system} - E_{gas}$, where $E_{system+gas}$ is the total energy for the sheet with the gas adsorbed, $E_{system}$ and $E_{gas}$ are the energies only for the sheets and the gases respectively.

The optimized boron monolayer structure is shown in Fig. 4.3, where the unit cell contains 14 atoms (shown within the dashed lines). The lattice constants are 5.85 Å and 6.67 Å. The BS is functionalized with dope atoms, C, N, S, P and Li in a study of the HER and OER. The most stable configurations were found trying different doping sites. Boron atoms in a BS have either 5 or 6 coordination number (CN) and it has been found that if 5 CN boron atom is replaced, it leads to the most stable configuration.
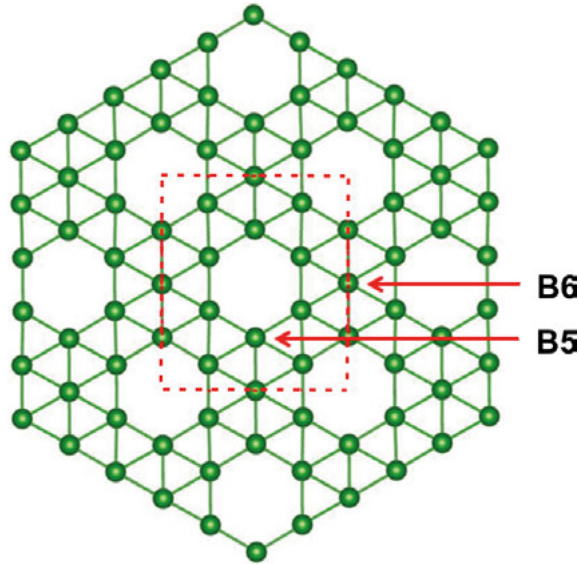


*Figure 4.3.* The unit cell of the boron sheet is shown within the dashed lines. B5 and B6 represent sites with coordination number 5 and 6 respectively.

In Table 4.3 the bond length between the impurity atoms and the boron atoms with 5 CN (B5-X) an 6 CN (B6-X) are presented. These bond length differ from the bonds in the pristine BS, where bonds with 5 CN and 6 CN have the same bond length (1.68 Å); the dope atoms displace the nearest and second nearest neighbours.

| | BS | C | N | S | P | Li |
|---|---|---|---|---|---|---|
| $E_H(eV)$ | -2.47 | -3.22 | -3.89 | -3.61 | -5.73 | -3.64 |
| $E_O(eV)$ | -1.74 | -2.21 | -3.93 | -4.66 | -4.39 | -3.99 |
| $\Phi(eV)$ | 4.22 | 4.18 | 4.42 | 4.49 | 4.11 | 4.41 |
| B5-X(Å) | | 1.61 | 1.59 | 1.91 | 1.77 | 1.80 |
| B6-X(Å) | | 1.655 | 1.644 | 1.768 | 1.888 | 2.403 |

**Table 4.3.** *The workfunctions and the adsorption energies of hydrogen and oxygen on pristine and doped BS. The bond length for each dope atom to 5 CN and 6 CN boron atom respectively.*

Fig. 4.4 shows the pristine and doped BS with the hydrogen and oxygen gas molecules adsorbed the surface. It shows that the most favorable sites for hydrogen adsorption are at the top site of a boron atom having 5 CN (Li doped BS) and boron atom having 6 CN (pristine, C and P doped BS). In the oxygen case the most favorable sites are at the bridge sites (between boron atoms with 5 CN and 6 CN) (pristine and Li doped BS), on the top site of carbon and molecule binds at the hollow between boron atoms with 5 CN and on top of the
 Adsorption energies and workfunction are shown in Table 4.3. It shows that both hydrogen and oxygen bind strongly to all the systems. For the good HER hydrogen adsorption energy should be close to 0.33 eV and close to 0.24 eV for the good OER, which shows that the pristine and carbon doped BS are the most promising candidates for both the HER and the OER. The investigation from calculated DOS show a metallic behavior for the doped systems Fig. 4.5. The optical absorption spectra for the pristine and doped boron sheets (BS) are shown in Fig. 4.6. The spectra from pristine BS show several adsorption peaks at 1.26, 2.67, 6.50 and 9.38 eV, which gives response in the visible range. The doped system show the largest adsorption peaks at low photon energy. [33–39]
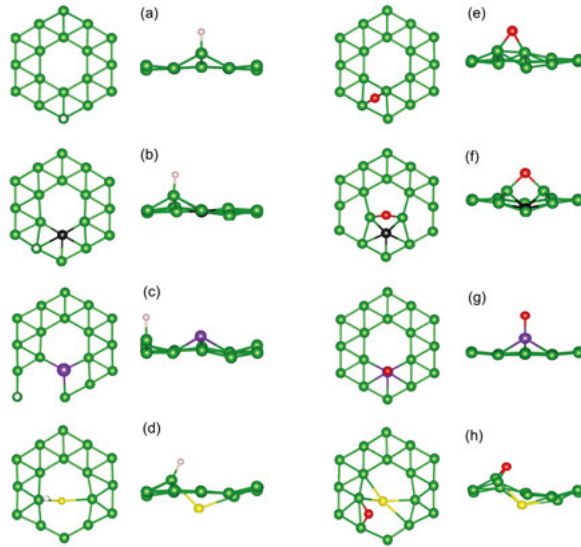
*Figure 4.4.* The two left columns (a)-(d) show the optimized structure of pristine and functionalized boron sheet. Each structure has hydrogen (the white ball) adsorbed to them at the preferable site. In the two right columns the same is shown for oxygen (the red ball) adsorption. The dopants are C (black), P (purple) and Li (yellow).
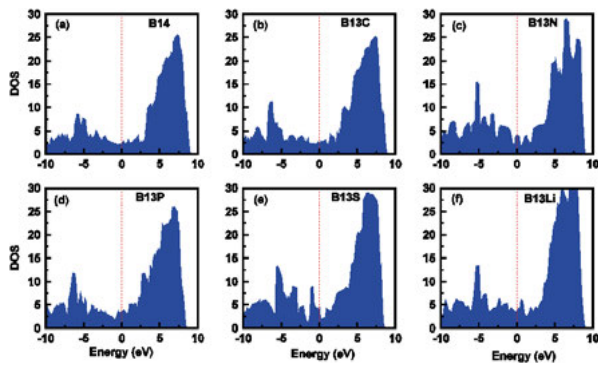


*Figure 4.5.* The total DOS of pristine and functionalized boron sheets. The dopants are C, N, P, S and Li.

## 4.3 Two-dimensional Boron Monolayer for Sensing Application

As band structure and the band edge alignment is the essence behind the investigation of photocatalytic materials, the same philosophy can be envisaged in the gas sensing application, where the gas molecules could be sensed or
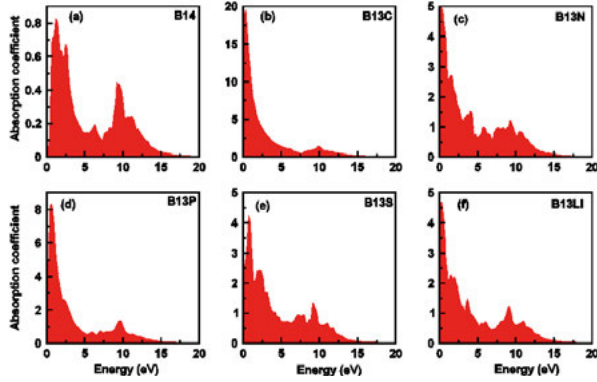
*Figure 4.6.* The absorption spectra for pristine and functionalized boron sheets are shown with the dopants C, N, P, S and Li.

detected with respect to the band gap changes in the materials. In this regard, boron monolayer can also be used for gas sensing applications, because of its large surface to volume ratio along with the charge transfer from gas to surface or surface to gas. In addition to graphene, other 2D materials have been investigated for their suitability in gas sensing application like silicene, $MoS_2$, phosphorene [40–44]. Borophene is the boron equivalent to graphene [45–47] and it has been studied for electronic and optical properties[48] It has been investigated for applications like anode material in Li and Na ion batteries as well. [49–51]

The DFT based electronic structure calculation has been done meassuring the directional dependence of the electronic transport properties [52] and $NH_3$ has been examined on the boron based nanostructure $B_40$ fullerene. [53] So in this paper we wanted to investigate borophene even further as a gas sensor for the gas molecules CO, $CO_2$, NO, $NO_2$ and $NH_3$ (Fig. 4.7). In this work, we have performed DFT based investigations to find the preferable orientations, arrangements together with binding energies for the gas adsorption on the boron monolayer surface. For the sensing application, we have investigated the transmission function and determined the corresponding I-V curves using the non-equilibrium Green's function (NEGF) [54] [55] formalism.

We have found that as compared to the other 2D materials such as phosphorene, graphene and $MoS_2$,the binding of the gases with borophene are much superior and the amount of charge transfer show better sensitivity. It has also been found that the adsorption of different gases lead to the large transmis-
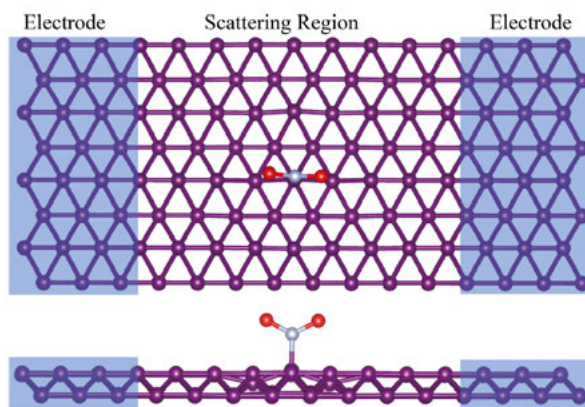
*Figure 4.7.* The borophene monolayer set up for the gas sensing application

sion function for each of the gases. Thus borophene monolayer has also been emerged as a realistic gas sensor device with distinct ON and OFF states.

## 4.4 Two-dimensional $Mg_3N_2$ Monolayer for HER Mechanism

In the quest for efficient 2D catalytic materials, we have subsequently envisaged $Mg_3N_2$ monolayer particularly for hydrogen evolution reaction based on electronic structure calculations within DFT framework. The $Mg_3N_2$ monolayer is having a hexagonal two-dimensional structure with a lattice constant of 6.8316 Å$\times$ 6.8316 Åwith 1.972 Åas Mg-N bond-length. We have performed electronic structure calculations for pristine $Mg_3N_2$ monolayer in the form of $3 \times 3$ supercell (Fig. 4.8).

The reaction coordinate (Fig. 4.9) is a deterministic way to compare the HER catalytic activity of different systems. The idea is to compare the adsorption free energy, $\Delta G$, for the intermediates of HER, $H^+ + e^-$, $H^*$ and $1/2H_2$ (* denotes that H is adsorbed to the surface of the material.) The difference in adsorption free energies needs to be closed to zero for a optimal HER catalyst. In this work, we have determined the hydrogen adsorption free energy for different adsorption sites, while comparing the results with the platinum case, which is the best HER catalyst till date.

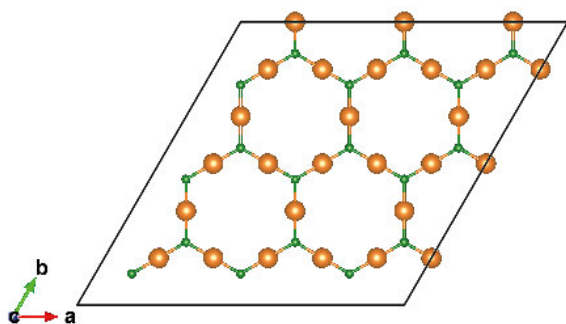The Density of States (DOS) calculation (Fig. 4.10) for the pristine $Mg_3N_2$

38

*Figure 4.8.* The $3 \times 3$ supercell of the $Mg_3N_2$ 2D material, green balls are nitrogen and orange are magnesium.
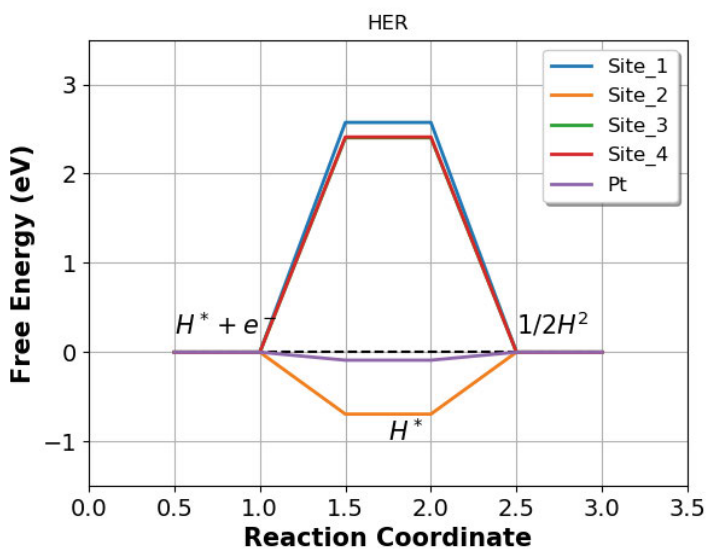


*Figure 4.9.* Reaction coordinates for hydrogen adsorption in different sites on a $Mg_3N_2$ 2D material compared to hydrogen adsorption on a platinum surface.

monolayer shows semiconducting nature with a bandgap of 1.69 eV, which is in the visible range of solar spectrum. From the DOS, one can observe HOMO, LUMO and Fermi level as at -3.99 eV, -2.31 eV and -3.15 eV respectively. The hydrogen adsorption has been found to be occurring most likely

due to the $s - p$ hybridization, as the $p$ states of N atoms are most prominent below the Fermi level. The overlap of $N - p$ states orbitals with $Mg - s$ orbitals around -6.13 eV together with $Mg - p$ states have been observed. In general, the HER takes place while the electrons are getting extracted from the material, and therefore the lower workfunction often leads to the better catalytic property. All the values of workfunction, Fermi level and bandgap of the considered systems are depicted Table 4.4.
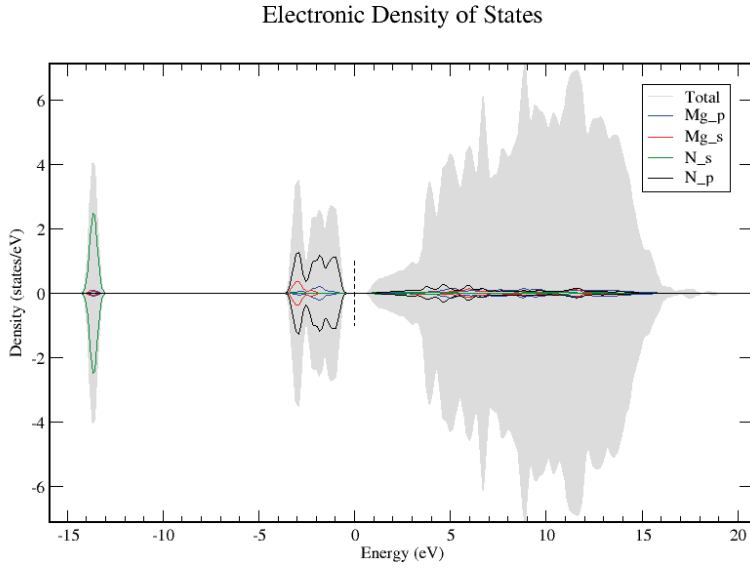


*Figure 4.10.* Density of States for the pristine $Mg_3N_2$ monolayer. Total DOS is displayed by the gray area, whereas the $Mg - p$, $Mg - s$, $N - s$ and $N - p$ states are depicted by the blue, red, green and black lines.

| System | Work function (eV) | Fermi level (eV) | Bandgap (eV) |
|---|---|---|---|
| Pristine sheet | 3.96 | -3.14 | 1.69 |
| 1H | 3.59 | -2.71 | - |
| 2H | 3.74 | -2.86 | 0.79 |
| 4H | 3.35 | -2.34 | 0.17 |
| 6H | 3.04 | -2.11 | 0.32 |

**Table 4.4.** *Work functions, Fermi levels and Bandgap for the pristine, 1H, 2H, 4H and 6H systems.*

Further, we have determined the hydrogen adsorption energies for different number of hydrogen atoms adsorbing on different favourable adsorption sites.

Table 4.5 shows the associated adsorption energies for 1H, 2H, 4H and 6H adsorptions, where it has been found that hydrogen tends to adsorb only on the nitrogen site in the pristine 2D structure. For a optimal HER catalyst, the binding of hydrogen with the corresponding substrate should not be too strong or too week. In this connection, Fig. 4.11 shows the best adsorption sites for 1H, 2H, 4H and 6H adsorption.

| Number of Hydrogen at $N^{th}$ site | Total energy (eV) | Adsorption energy (eV) | Binding energy /Hydrogen atom (eV) |
|---|---|---|---|
| 1H on $1^{st}$ site | -186.626 | 2.333 | 2.334 |
| 1H on $2^{nd}$ site | -189.894 | -0.934 | -0.934 |
| 1H on $3^{rd}$ site | -186.79848 | 2.16203763 | 2.162 |
| 1H on $4^{th}$ site | -186.790 | 2.170 | 2.170 |
| 2H on $1^{st}$ site | -194.238 | -1.892 | -0.946 |
| 2H on $2^{nd}$ site | -193.198 | -0.853 | -0.427 |
| 2H on $3^{rd}$ site | -194.261 | -1.914 | -0.957 |
| 4H on $1^{st}$ site | -202.541 | -3.425 | -0.856 |
| 4H on $2^{nd}$ site | -202.856 | -3.741 | -0.935 |
| 4H on $3^{rd}$ site | -202.427 | -3.311 | -0.828 |

**Table 4.5.** *Total energy, binding energy and binding energy (eV) / H atom for hydrogen adsorption with different number of atoms and on different sites.*

The determined density of states (DOS), work function, Fermi level and Bandgap are depicted in Fig. 4.12 for the non pristine structures. We can observe that the work function for the pristine structure is slightly higher ($\approx$4 eV) as compared to the systems with hydrogen ($\approx$3.5 eV), however in the case of 6H adsorption, the corresponding value getting decreased ($\approx$3 eV). The corresponding Fermi level has been shifted from -3.1455eV (pristine) to -2.1126eV for 6H adsorption case. The band gap change for different number of H adsorption has also been depicted in Table 4.4.
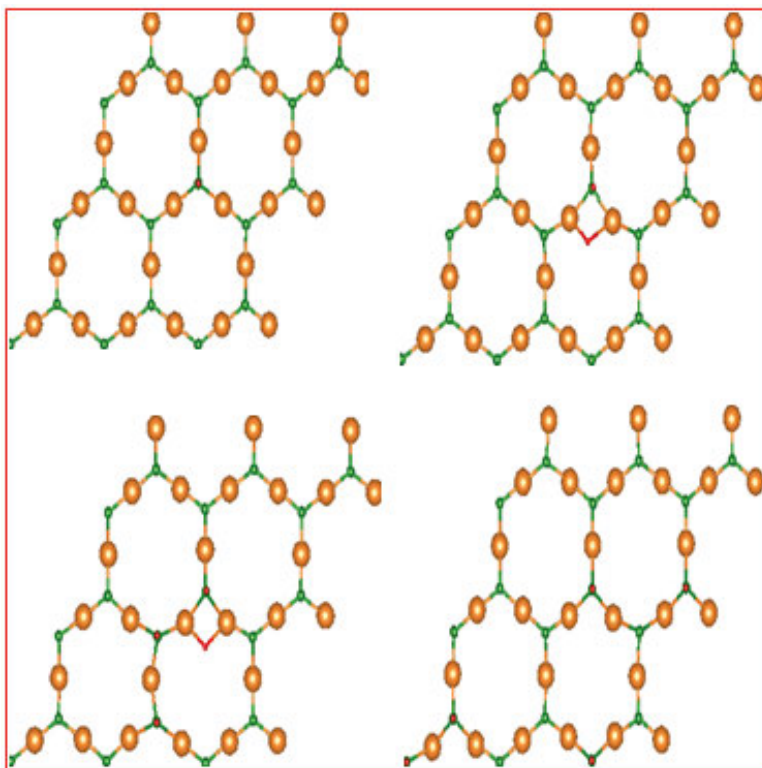
*Figure 4.11.* $Mg_3N_2$ supercell with 1H, 2H, 4H and 6H adsorbed on the surface of the 2D material.

The charge transfer between the catalytic material and the hydrogen atom is also one of the decisive factors, as it has been represented in the form of charge difference for various cases in Figure 4.13. With the help of Bader charge analysis, as shown in table 4.6, we can explain the charge difference for the constituent atoms of the monolayer (Mg and N average charge), which can also imply the hydrogen adsorption on the favourable adsorption sites.
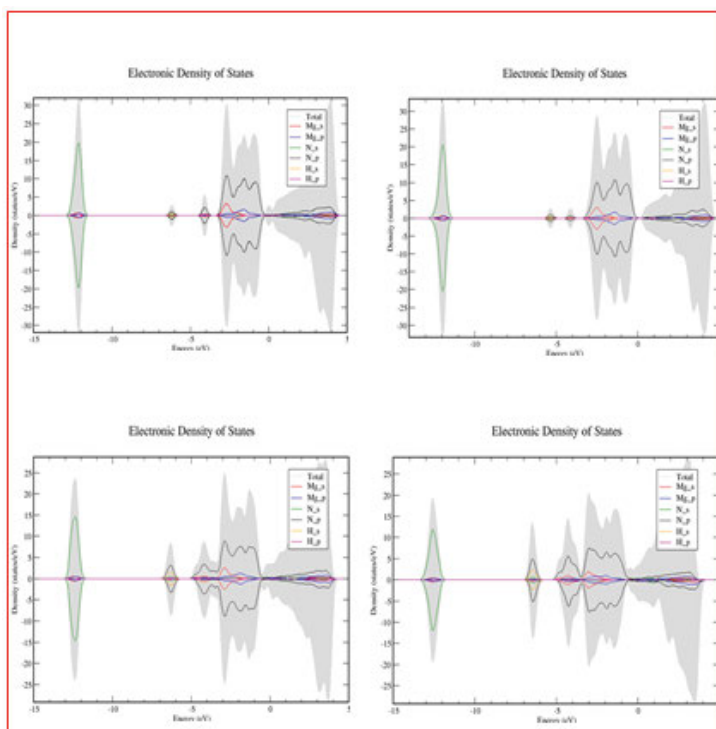
*Figure 4.12.* The Density of State for 1H, 2H, 4H and 6H adsorption cases

We have observed that in case of 1H, the hydrogen atom is acquiring a positive net charge (+0.321 e) with the nitrogen atom associated with the hydrogen adsorption (acceptor 1) with a positive charge difference (+0.186 e) as compared to the average charge for nitrogen. Moreover, it can be seen that the negative charge is distributed around the neighbouring nitrogen atoms making the nitrogen atoms with more negative average charge (-0.007 e) while the magnesium atoms are becoming less positive average charge (-0.007 e) as compared to the pristine $Mg_3N_2$ case. For the 2H case the situation is similar,

| System/element | Mg | N | N acceptor 1 | N acceptor 2 | H |
|---|---|---|---|---|---|
| $Mg_3N_2$ | 1.510 | -2.246 | - | - | - |
| $Mg_3N_2$+1H | 1.503 | -2.253 | -2.067 | - | 0.321 |
| $Mg_3N_2$+2H | 1.491 | -2.252 | -2.044 | -2.018 | 0.310 |

**Table 4.6.** *The average net charge for the elements and the net charge for the acceptor nitrogen atoms.*
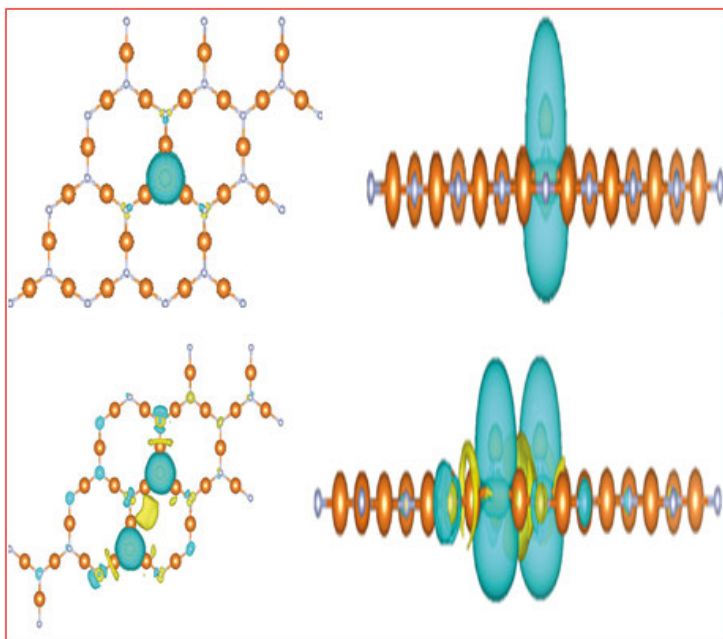
*Figure 4.13.* The charge difference for 1H and 2H, bird's eye and side view.

however the negative charge is less distributed on the neighbouring magnesium and nitrogen atoms. Therefore, the magnesium atoms have less positive average charge (-0.019 e) , while the nitrogen atoms have a more negative average charge (-0.008 e). The hydrogen atoms are having average net charge (+0.310 e), while the nitrogen atoms are having positive charge difference (+0.208 e and +0.234 e) as compared to the average charge. [56–65]

# 5. Summary and Future Outlook

In summary of the catalytic activity investigation of $PtS_2$ and $WS_2$, we have tuned the HER catalytic activity of both the monolayers by electronic structure calculations based on the density functional theory (DFT). We have systematically investigated the effect of foreign elements, such as Ag, Au, Hg, Pd, Ir, Rh, and Rh, on the catalytic activity of these two monolayers. We have also demonstrated that the van der Waals (VDW) interactions are important enough to accurately predict the adsorption energy on the individual catalytic surfaces. The band structure has been determined using hybrid exchange correlation functional with spin-orbit coupling. $PtS_2$ is an indirect band gap semiconductor, whereas $WS_2$ exhibits a direct band gap. The DOS has been calculated to predict the effect of dopant on the band gap. To find the optimal photocatalytic activity, we have functionalized these materials with a series of transition metals, such as Ru, Rh, Pd, Ag, Ir, Au, and Hg. The electronic structure calculations of pristine and functionalized $PtS_2$ and $WS_2$ show that among all systems considered, the Pd doped $WS_2$ system shows the optimal binding energy of $H_2$ for the catalytic activity in the HER.

DFT based electronic structure calculations within PBE functional have also been performed to explore the structural, electronic, and optical properties of the pristine as well as functionalized (with C, N, P, S, and Li) boron monolayer. The DOS calculations predict the metallic nature of the considered systems, while the optical spectra are found to display the absorption peaks at low photon energies. From the calculated adsorption energies of hydrogen and oxygen, it has been found that both hydrogen and oxygen are strongly bound to the surfaces of pristine and functionalized BS. The hydrogen atom is found to be most stable at the top site on the six coordinated B atom for pristine, C and P doped and on the five coordinated B atom for Li doped BS, while the O atom is found to be stable at the bridge site for pristine and Li doped BS, hollow site for C and on the top site for P doped BS. We have also found that among all the functionalization cases, C-doped Boron monolayer has been emerged as the promising most candidate after pristine BS to show HER and OER activity.

The future direction is to investigate novel 2D materials for example $B_2C$ to envisage the HER and OER activity based on the reaction coordinate. To construct the reaction coordinate for OER would be a real challenge, which we will pursue in near future. We want to explore how the transport of electrons

can be correlated with the catalytic reaction mechanism in 2D materials. We would like to predict novel 2D materials and subsequently investigating their catalytic activities from the perspective of HER and OER, which could be validated in the experimental synthesis condition.

# 6. Sammanfattning på svenska

I den här avhandlingen har verktyg och metoder som är sammanlänkade med densitetsfunktionalteori (DFT) använts för att förutsäga den katalytiska effekten hos tvådimensionella (2D) nanomaterial för använding inom vätgasproduktion med vatten som råmaterial och solljuset som energikälla, så kallad fotokatalytisk vattensplittring.

Arbetet omfattar en grundläggande beskrivning av teorin som är DFT från Schrödingerekvationen med teorier och definitioner av en fullskalig flerpartikels-Hamiltonian genom Born-Oppenheimer-approximationen, Hohenberg-Kohn-teoremen och Kohn-Shams sats till den gällande densitetsfunktionalteorin. Beskrivningen tar upp definitioner och härledningar av pseudopotentialer, energiutbytesfunktionaler, samt vertyg och metoder som använts. *Med Schrödingerekvationen beräknas energin hos en molekyl, ett material eller ett 2D-material genom att beräkna krafterna mellan atomer, protoner, elektroner och mellan dem själva. I DFT ersätts elektronerna med en elektrondensitet, som beräknas för varje atomkonfiguration. Sedan jämförs resultaten för att finna den konfiguration som har den lägsta energin, dvs man löser Schrödingerekvationen genom att minimera energin. Från den slutgiltiga elektrondensiteten kan fysikaliska storheter beräknas.* Vidare kommer en redogörelse av innebörden av fotokatalism. Här berättas det om vattensplittringens två delreaktioner Hydrogen evolution reaction (HER) och Oxygen evolution reaction (OER), dvs hur vätgas ($H_2$) och syrgas ($O_2$) bildas från vattenmolekyler ($H_2O$). Poängen med användandet av en katalysator förklaras, vilket är att sänka den elektrokemiska potentialen så att energin från solljuset är tillräckligt för att bryta de kemiska bindningarna i vattenmolekylen ungefär som hur en katalysator i en bil bryter bindningarna i CO- och NO-molekylerna för att bilda koldioxid ($CO_2$) och kvävedioxid ($NO_2$). Varför 2D-material kan vara goda substitut till ädelmetaller förklaras genom att visa vad som katagoriserar en optimal katalysator, saker som bandgap (HOMO och LUMO), adsorptionsenergier för väteatomen och syreatomen, absorbtionsspekra, m.m. Att man dessutom kan

enkelt kan dopa 2D-material genom att byta ut en eller flera atomer med antingen främmande atomslag eller vakanser och på så sätt manipulera bandgap, adsorbtionsenergier, etc, visas också. Slutligen berättas hur man kan använda DFT för att bestämma funktionaliteten hos ett specifikt material genom att definiera den fria energin hos respektive gasmolekyl i den adsorberade fasen när reaktionen befinner sig i jämviktsläget och hur man beräknar den utifrån adsorptionsenergin. *Det man gör är jämförelser av energin hos olika system, med eller utan adsorberade atomer, med eller utan dopatomer och vakanser. Dessutom jämförs resultaten med en referens (i fallet vattensplittring (både HER och OER) jämför man ofta med platinum.* I nästkommande kapitel visas bilder, grafer och resultatdata från undersökningen av diverse material från artiklarna, vilka den här avhandlingen bygger på. Varpå följande kapitel sammanfattar arbetet och drar slutsatser av resultaten. Sist av allt kommer artiklarna och manuskripten i sin fulla form.

# 7. Acknowledgment

First of all, I would like to thank my supervisor Prof. Rajeev Ahuja for given me the opportunity to join his group in the division of Materials Theory at Uppsala University by accepting my application and for not firering me the first week and all the weeks after that. ;-) I would also like to thank him for all his help he has given to me. I would like to especially thank my co-supervisor Dr. Sudip Chakraborty for his help with my research and all the fruitful discussions during the writing of my thesis and his encouragement for last three years. I also thank my other two co-supervisors, Dr. Anton Grigoriev and Dr. Henrik Ottosson. I would like to thank all my collaborators and colleagues for working together with me on projects, especially Amitava Banerjee, Vivekanand Shulka, Naresh Kumar Jena. All the colleagues and friends for letting me join them for lunches, coffee breaks, beer nights, etc. Thank you Robert Johansson, Jonathan Chico, Kostas Koumpouras, Alecos Aperis and Marco Berritta, Ritwik Mondal, Amitava Banerjee and Sudip Chakraborty among others for the discussions and for listening to my long winded explanations and anecdotes. Thank you Cleber and Claudia Marchiori, Emil Edin, Teeraphat Watcharatharapong (Non), Jose Luis Silva, Rodrigo De Carvalho, Xiao Yang and Rafael Araujo Café Ångström and Unico wouldn't have been the same without you. An extra thanks to my office mates Rafael Araujo, Amitava Banerjee, Thanayut Kaewmaraya (M), Xiao Yang, Juan David Vasquez Jaramillo and Ekaterina Anikina (Kate), who took time out of their busy schedule to help me and answering my questions. Thank Robert Johansson and Fredrik Fransson for being such a good friends since highschool through my master studies and beyond, an extra thanks to Robert for helping me get this job and for all the help during my PhD studies. Thank you to people who studied in Linköping together with me, Gustav Åström, Robert Johansson, Martin Svensson, Martin Lundgren and Mark Kesper among others. Thank you Martin Svensson and Sara Fagerberg for being the hosts and inviting us over for game nights, etc, which made us forget our the monotonous and boring lifes

for awile. Finally thanks to my family and dear friends from my childhood and beyond, to my best childhood friend Tobias Staberg.

# References

[1] Andreas Züttel, Arndt Remhof, Andreas Borgschulte, and Oliver Friedrichs. Hydrogen: the future energy carrier. *Philosophical Transactions of the Royal Society of London A: Mathematical, Physical and Engineering Sciences*, 368(1923):3329–3342, 2010.

[2] Jonas Ångström, Robert Johansson, Line Holdt Rude, Carsten Gundlach, Ralph H. Scheicher, Rajeev Ahuja, Olle Eriksson, Torben R. Jensen, and Martin Sahlberg. Hydrogen storage properties of the pseudo binary laves phase $(Sc_{1-x}Zr_x)(Co_{1-y}Ni_y)_2$ system. *International Journal of Hydrogen Energy*, 38(23):9772 – 9778, 2013.

[3] Andreas Züttel. Hydrogen storage methods. *Naturwissenschaften*, 91(4):157–172, 2004.

[4] Canan Acar, Ibrahim Dincer, and Greg F. Naterer. Review of photocatalytic water-splitting methods for sustainable hydrogen production. *International Journal of Energy Research*, 40(11):1449–1473, 2016. ER-16-6611.R1.

[5] Peter C. K. Vesborg, Brian Seger, and Ib Chorkendorff. Recent development in hydrogen evolution reaction catalysts and their practical implementation. *The Journal of Physical Chemistry Letters*, 6(6):951–957, 2015. PMID: 26262851.

[6] Nian-Tzu Suen, Sung-Fu Hung, Quan Quan, Nan Zhang, Yi-Jun Xu, and Hao Ming Chen. Electrocatalysis for the oxygen evolution reaction: recent development and future perspectives. *Chem. Soc. Rev.*, 46:337–365, 2017.

[7] Yunguo Li, Yan-Ling Li, Baisheng Sa, and Rajeev Ahuja. Review of two-dimensional materials for photocatalytic water splitting from a theoretical perspective. *Catal. Sci. Technol.*, 7:545–559, 2017.

[8] Aamar F. Khan, Michael P. Down, Graham C. Smith, Christopher W. Foster, and Craig E. Banks. Surfactant-exfoliated 2d hexagonal boron nitride (2d-hbn): role of surfactant upon the electrochemical reduction of oxygen and capacitance applications. *J. Mater. Chem. A*, 5:4103–4113, 2017.

[9] Yuanyue Liu, Evgeni S. Penev, and Boris I. Yakobson. Probing the synthesis of two-dimensional boron by first-principles computations. *Angewandte Chemie International Edition*, 52(11):3156–3159, 2013.

[10] Boubekeur Lalmi, Hamid Oughaddou, Hanna Enriquez, Abdelkader Kara, Sébastien Vizzini, Bénidicte Ealet, and Bernard Aufray. Epitaxial growth of a silicene sheet. *Applied Physics Letters*, 97(22):223109, 2010.

[11] W. Kohn and L. J. Sham. Self-consistent equations including exchange and correlation effects. *Phys. Rev.*, 140:A1133–A1138, Nov 1965.

[12] J. P. Perdew, K. Burke, and M. Ernzerhof. Generalized gradient approximation made simple. *Phys. Rev. Lett.*, 77:3865–3868, 1996.

[13] J. P. Perdew, K. Burke, and M. Ernzerhof. Erratum: Generalized gradient approximation made simple. *Phys. Rev. Lett.*, 78:1396, 1997.

[14] D. R. Hamann, M. Schlüter, and C. Chiang. Norm-conserving pseudopotentials. *Phys. Rev. Lett.*, 43:1494–1497, Nov 1979.

[15] Vladimir I. Anisimov, Jan Zaanen, and Ole K. Andersen. Band theory and mott insulators: Hubbard u instead of stoner i. *Phys. Rev. B*, 44:943–954, Jul 1991.

[16] Matthias Ernzerhof and Gustavo E. Scuseria. Assessment of the perdew-burke-ernzerhof exchange-correlation functional. *The Journal of Chemical Physics*, 110(11):5029–5036, 1999.

[17] John P. Perdew, Matthias Ernzerhof, and Kieron Burke. Rationale for mixing exact exchange with density functional approximations. *The Journal of Chemical Physics*, 105(22):9982–9985, 1996.

[18] Kieron Burke, Matthias Ernzerhof, and John P. Perdew. The adiabatic connection method: a non-empirical hybrid. *Chemical Physics Letters*, 265(1):115 – 120, 1997.

[19] Lars Hedin. New method for calculating the one-particle green's function with application to the electron-gas problem. *Phys. Rev.*, 139:A796–A823, Aug 1965.

[20] J. K. Nørskov, J. Rossmeisl, A. Logadottir, L. Lindqvist, J. R. Kitchin, T. Bligaard, and H. Jónsson. Origin of the overpotential for oxygen reduction at a fuel-cell cathode. *The Journal of Physical Chemistry B*, 108(46):17886–17892, 2004.

[21] J. Rossmeisl, A. Logadottir, and J.K. Nørskov. Electrolysis of water on (oxidized) metal surfaces. *Chemical Physics*, 319(1):178 – 184, 2005. Molecular Charge Transfer in Condensed Media - from Physics and Chemistry to Biology and Nanoengineering in honour of Alexander M. Kuznetsov on his 65th birthday.

[22] J. Rossmeisl, Z.-W. Qu, H. Zhu, G.-J. Kroes, and J.K. Nørskov. Electrolysis of water on oxide surfaces. *Journal of Electroanalytical Chemistry*, 607(1):83 – 89, 2007. Theoretical and Computational Electrochemistry.

[23] P. Hohenberg and W. Kohn. Inhomogeneous electron gas. *Phys. Rev.*, 136:B864–B871, Nov 1964.

[24] P. E. Blöchl. Projector augmented-wave method. *Phys. Rev. B*, 50:17953–17979, 1994.

[25] Thomas D. Kühne, Matthias Krack, Fawzi R. Mohamed, and Michele Parrinello. Efficient and accurate car-parrinello-like approach to born-oppenheimer molecular dynamics. *Phys. Rev. Lett.*, 98:066401, Feb 2007.

[26] Sudip Chakraborty, Amitava Banerjee, Teeraphat Watcharatharapong, Rafael B Araujo, and Rajeev Ahuja. Current computational trends in polyanionic cathode materials for li and na batteries. *Journal of Physics: Condensed Matter*, 30(28):283003, jun 2018.

[27] Hendrik J. Monkhorst and James D. Pack. Special points for brillouin-zone integrations. *Phys. Rev. B*, 13:5188–5192, Jun 1976.

[28] Xiaoxin Zou and Yu Zhang. Noble metal-free hydrogen evolution catalysts for water splitting. *Chem. Soc. Rev.*, 44:5148–5180, 2015.

[29] Marc T.M. Koper. Thermodynamic theory of multi-electron transfer reactions: Implications for electrocatalysis. *Journal of Electroanalytical Chemistry*, 660(2):254 – 260, 2011. Physics and Chemistry of Charge Transfer in Condensed Media.

[30] Stefan Grimme. Semiempirical gga-type density functional constructed with a long-range dispersion correction. *Journal of Computational Chemistry*, 27(15):1787–1799.

[31] Jochen Heyd, Gustavo E. Scuseria, and Matthias Ernzerhof. Hybrid functionals based on a screened coulomb potential. *The Journal of Chemical Physics*, 118(18):8207–8215, 2003.

[32] Aparna Ganguly, Oruganti Anjaneyulu, Kasinath Ojha, and Ashok K. Ganguli. Oxide-based nanostructures for photocatalytic and electrocatalytic applications. *CrystEngComm*, 17:8978–9001, 2015.

[33] Xiaojun Wu, Jun Dai, Yu Zhao, Zhiwen Zhuo, Jinlong Yang, and Xiao Cheng Zeng. Two-dimensional boron monolayer sheets. *ACS Nano*, 6(8):7443–7453, 2012. PMID: 22816319.

[34] Süleyman Er, Gilles A. de Wijs, and Geert Brocks. Dft study of planar boron sheets: A new template for hydrogen storage. *The Journal of Physical Chemistry C*, 113(43):18962–18967, 2009.

[35] Hui Tang and Sohrab Ismail-Beigi. First-principles study of boron sheets and nanotubes. *Phys. Rev. B*, 82:115412, Sep 2010.

[36] Hui Tang and Sohrab Ismail-Beigi. Novel precursors for boron nanotubes: The competition of two-center and three-center bonding in boron sheets. *Phys. Rev. Lett.*, 99:115501, Sep 2007.

[37] G. Kresse and D. Joubert. From ultrasoft pseudopotentials to the projector augmented-wave method. *Phys. Rev. B*, 59:1758–1775, Jan 1999.

[38] M. Gajdoš, K. Hummer, G. Kresse, J. Furthmüller, and F. Bechstedt. Linear optical properties in the projector-augmented wave methodology. *Phys. Rev. B*, 73:045112, Jan 2006.

[39] Teck L. Tan, Lin-Lin Wang, Duane D. Johnson, and Kewu Bai. A comprehensive search for stable ptâpd nanoalloy configurations and their use as tunable catalysts. *Nano Letters*, 12(9):4875–4880, 2012. PMID: 22894175.

[40] F Schedin, AK Geim, SV Morozov, EW Hill, P Blake, MI Katsnelson, and KS Novoselov. Detection of individual gas molecules adsorbed on graphene. *Nature materials*, 6(9):652, 2007.

[41] O. Leenaerts, B. Partoens, and F. M. Peeters. Adsorption of $h_2O$, $Nh_3$, co, $No_2$, and no on graphene: A first-principles study. *Phys. Rev. B*, 77:125416, Mar 2008.

[42] Liangzhi Kou, Aijun Du, Changfeng Chen, and Thomas Frauenheim. Strain engineering of selective chemical adsorption on monolayer mos2. *Nanoscale*, 6:5156–5161, 2014.

[43] Liangzhi Kou, Thomas Frauenheim, and Changfeng Chen. Phosphorene as a superior gas sensor: Selective adsorption and distinct iâv response. *The Journal of Physical Chemistry Letters*, 5(15):2675–2681, 2014. PMID: 26277962.

[44] Jariyanee Prasongkit, Rodrigo G. Amorim, Sudip Chakraborty, Rajeev Ahuja, Ralph H. Scheicher, and Vittaya Amornkitbamrung. Highly sensitive and selective gas detection based on silicene. *The Journal of Physical Chemistry C*, 119(29):16934–16940, 2015.

[45] Manish Chhowalla, Hyeon Suk Shin, Goki Eda, Lain-Jong Li, Kian Ping Loh, and Hua Zhang. The chemistry of two-dimensional layered transition metal dichalcogenide nanosheets. *Nature chemistry*, 5(4):263, 2013.

[46] Andrew J. Mannix, Xiang-Feng Zhou, Brian Kiraly, Joshua D. Wood, Diego Alducin, Benjamin D. Myers, Xiaolong Liu, Brandon L. Fisher, Ulises Santiago, Jeffrey R. Guest, Miguel Jose Yacaman, Arturo Ponce, Artem R. Oganov, Mark C. Hersam, and Nathan P. Guisinger. Synthesis of borophenes: Anisotropic, two-dimensional boron polymorphs. *Science*, 350(6267):1513–1516, 2015.

[47] Zhuhua Zhang, Evgeni S Penev, and Boris I Yakobson. Two-dimensional materials: polyphony in b flat. *Nature chemistry*, 8(6):525, 2016.

[48] Bo Peng, Hao Zhang, Hezhu Shao, Yuanfeng Xu, Rongjun Zhang, and Heyuan Zhu. The electronic, optical, and thermodynamic properties of borophene from first-principles calculations. *Journal of Materials Chemistry C*, 4(16):3592–3598, 2016.

[49] Chieh-Szu Huang. Adsorption of the gas molecules nh3, no, no2, and co on borophene. *The Journal of Physical Chemistry C*, 06 2018.

[50] Bohayra Mortazavi, Arezoo Dianat, Obaidur Rahaman, Gianaurelio Cuniberti, and Timon Rabczuk. Borophene as an anode material for ca, mg, na or li ion storage: A first-principle study. *Journal of Power Sources*, 329:456 – 461, 2016.

[51] Yang Zhang, Zhi-Feng Wu, Peng-Fei Gao, Sheng-Li Zhang, and Yu-Hua Wen. Could borophene be used as a promising anode material for high-performance lithium ion battery? *ACS Applied Materials & Interfaces*, 8(34):22175–22181, 2016. PMID: 27487298.

[52] José Eduardo Padilha, Roberto Hiroki Miwa, and Adalberto Fazzio. Directional dependence of the electronic and transport properties of 2d borophene and borophane. *Phys. Chem. Chem. Phys.*, 18:25491–25496, 2016.

[53] Bin Lin, Huilong Dong, Chunmiao Du, Tingjun Hou, Haiping Lin, and Youyong Li. B40 fullerene as a highly sensitive molecular device for nh3 detection at low bias: a first-principles study. *Nanotechnology*, 27(7):075501, 2016.

[54] Mads Brandbyge, José-Luis Mozos, Pablo Ordejón, Jeremy Taylor, and Kurt Stokbro. Density-functional method for nonequilibrium electron transport. *Physical Review B*, 65(16):165401, 2002.

[55] Jariyanee Prasongkit, Anton Grigoriev, Biswarup Pathak, Rajeev Ahuja, and Ralph H Scheicher. Transverse conductance of dna nucleotides in a graphene nanogap from first principles. *Nano letters*, 11(5):1941–1945, 2011.

[56] Jun Ho Shim, Youn Soo Kim, Minkyung Kang, Chongmok Lee, and Youngmi Lee. Electrocatalytic activity of nanoporous pd and pt: effect of structural features. *Phys. Chem. Chem. Phys.*, 14:3974–3979, 2012.

[57] Mårten E. Bjorketun, Alexander S. Bondarenko, Billie L. Abrams, Ib Chorkendorff, and Jan Rossmeisl. Screening of electrocatalytic materials for hydrogen evolution. *Phys. Chem. Chem. Phys.*, 12:10536–10541, 2010.

[58] Yunguo Li, Yan-Ling Li, Baisheng Sa, and Rajeev Ahuja. Review of two-dimensional materials for photocatalytic water splitting from a theoretical perspective. *Catal. Sci. Technol.*, 7:545–559, 2017.

[59] Aamar F. Khan, Michael P. Down, Graham C. Smith, Christopher W. Foster, and Craig E. Banks. Surfactant-exfoliated 2d hexagonal boron nitride (2d-hbn): role of surfactant upon the electrochemical reduction of oxygen and capacitance applications. *J. Mater. Chem. A*, 5:4103–4113, 2017.

[60] Yang Zhang, Zhi-Feng Wu, Peng-Fei Gao, Sheng-Li Zhang, and Yu-Hua Wen. Could borophene be used as a promising anode material for high-performance lithium ion battery? *ACS Applied Materials & Interfaces*, 8(34):22175–22181, 2016. PMID: 27487298.

[61] Peng-Fei Liu, Liujiang Zhou, Thomas Frauenheim, and Li-Ming Wu. A graphene-like mg3n2 monolayer: high stability, desirable direct band gap and promising carrier mobility. *Phys. Chem. Chem. Phys.*, 18:30379–30384, 2016.

[62] S. Harinipriya and M. V. Sangaranarayanan. Hydrogen evolution reaction on electrodes:â influence of work function, dipolar adsorption, and desolvation energies. *The Journal of Physical Chemistry B*, 106(34):8681–8688, 2002.

[63] Ding-Yuan Kuo, Jason K. Kawasaki, Jocienne N. Nelson, Jan Kloppenburg, Geoffroy Hautier, Kyle M. Shen, Darrell G. Schlom, and Jin Suntivich. Influence of surface adsorption on the oxygen evolution reaction on iro2(110). *Journal of the American Chemical Society*, 139(9):3473–3479, 2017. PMID: 28181433.

[64] Jae Yeong Cheon, Jong Hun Kim, Jae Hyung Kim, Kalyan C. Goddeti, Jeong Young Park, and Sang Hoon Joo. Intrinsic relationship between enhanced oxygen reduction reaction activity and nanoscale work function of doped carbons. *Journal of the American Chemical Society*, 136(25):8875–8878, 2014. PMID: 24911055.

[65] Aleksandar R. Zeradjanin, Ashokanand Vimalanandan, George Polymeros, Angel A. Topalov, Karl J. J. Mayrhofer, and Michael Rohwerder. Balanced work function as a driver for facile hydrogen evolution reaction â comprehension and experimental assessment of interfacial catalytic descriptor. *Phys. Chem. Chem. Phys.*, 19:17019–17027, 2017.

# Acta Universitatis Upsaliensis

*Digital Comprehensive Summaries of Uppsala Dissertations*
*from the Faculty of Science and Technology* 1804

Editor: The Dean of the Faculty of Science and Technology